

Dominating vs. Dominated: Generative Collapse in Diffusion Models

Hayeon Jeong, Jong-Seok Lee*

Yonsei University, Korea

{hayeon.jeong, jong-seok.lee}@yonsei.ac.kr

Abstract

Text-to-image diffusion models have drawn significant attention for their ability to generate diverse and high-fidelity images. However, when generating from multi-concept prompts, one concept token often dominates the generation, suppressing the others—a phenomenon we term the Dominant-vs-Dominated (DvD) imbalance. To systematically analyze this imbalance, we introduce DominanceBench and examine its causes from both data and architectural perspectives. Through various experiments, we show that the limited instance diversity in training data exacerbates the inter-concept interference. Analysis of cross-attention dynamics further reveals that dominant tokens rapidly saturate attention, progressively suppressing others across diffusion timesteps. In addition, head ablation studies show that the DvD behavior arises from distributed attention mechanisms across multiple heads. Our findings provide key insights into generative collapse, advancing toward more reliable and controllable text-to-image generation.

1. Introduction

Text-to-image diffusion models [9, 13, 21, 24, 25, 27, 39] have achieved remarkable success in generating high-quality images from textual descriptions. However, ensuring the model’s representational fidelity to textual concepts [38] remains a fundamental challenge. Recent research has extensively explored this limitation from complementary perspectives. One line of work investigates *memorization* [3, 5, 11, 12, 15, 26, 26, 28, 32, 33, 37], where models reproduce near-identical images across different random seeds mainly due to excessive duplication of specific image-prompt pairs in training data. Another line focuses on *image editing* [2, 8, 10, 22], aiming to enhance semantic compositional capability by addressing failures in generating images from complex prompts containing multiple diverse concepts.

*Corresponding author



Figure 1. Generation results for “Neuschwanstein Castle coaster” across five random seeds. Only one (SD 1.4) and two (SD 2.1) out of five seeds successfully generate both concepts.

In this work, we examine a complementary aspect that arises from the *interplay* of these two dimensions—training data characteristics and multi-concept compositional capability. We observe that when generating images from prompts containing multiple concepts, one concept can visually overwhelm the generation while the other is completely suppressed and fails to appear. For example, as shown in Fig. 1, when generating images from the prompt “Neuschwanstein Castle coaster” across different random seeds, the Castle’s distinctive architecture dominates nearly all outputs, while the coaster concept is entirely absent. In this paper, we refer to this as the *Dominant-vs-Dominated* (DvD) phenomenon.

DvD extends the existing understanding by operating at the *concept level through visual dominance*: unlike memorization, which concerns prompt-specific reproduction, and concept editing, which addresses semantic compositional failures, DvD reveals how an individual concept’s visual characteristics systematically suppress others during multi-concept generation. We hypothesize that this dominance emerges from *visual diversity disparity* in training data: concepts with limited variation (e.g., landmarks, artists) develop rigid visual priors, while high-diversity concepts (e.g., everyday objects) develop flexible representations. Through a controlled experiments using DreamBooth [29] to manipulate visual diversity, we show that the dominance

increases monotonically as the training diversity decreases, validating visual diversity disparity as the root cause.

To systematically investigate how DvD manifests, we propose DominanceBench, a curated benchmark of 300 prompts exhibiting strong DvD behavior. Through cross-attention analysis, we reveal that (1) DvD prompts exhibit significantly higher attention concentration on dominant tokens in lower-resolution layers at early denoising steps, (2) dominated concepts experience sharp attention decline in the early phase of denoising process, and (3) unlike memorization which localizes to specific heads, DvD emerges from distributed cooperation among multiple attention heads.

Our main contributions are:

- We characterize the Dominant-vs-Dominated (i.e., DvD) phenomenon and demonstrate through controlled experiments that visual diversity disparity in training data is its root cause.
- We propose DominanceBench, a benchmark dataset for systematic analysis of DvD across concept categories.
- We reveal the internal mechanisms of DvD through comprehensive cross-attention analysis, identifying when (early timesteps), where (lower-resolution layers), and how (distributed across heads) dominance manifests during generation.

2. Related Work

2.1. Memorization in Diffusion Models

Memorization in diffusion models refers to the phenomenon where models replicate near-identical training images during generation, raising significant privacy and copyright concerns [3, 33]. To understand how memorization is encoded in model architectures, researchers have examined cross-attention mechanisms from multiple perspectives, revealing imbalanced attention focus in token embeddings [5, 26], prediction magnitudes [37], and localized neurons [11].

Recent work has further investigated the root causes: [28] provided a geometric framework relating memorization to data manifold dimensionality, and [15] revealed that overestimation during early denoising collapses trajectories toward memorized images. While these works focus on detecting and preventing prompt-specific reproduction of entire training images, our work investigates how visual diversity disparity in training data leads to concept-level dominance in multi-concept generation.

2.2. Multi-concept Generation

Text-to-image diffusion models continue to face substantial difficulties when prompts contain multiple concepts—such as several objects, attributes, or artistic styles—often yielding attribute leakage, concept mixing, or incomplete sub-

jects. These limitations have been widely reported across compositional diffusion and attention-guided control frameworks [4, 6, 10, 16, 19, 34, 36], which show that even strong diffusion backbones tend to violate object–attribute bindings or collapse distinct entities. Recently, multi-concept customization and multi-subject generation approaches—including MC² [14], FreeCustom [8], Custom Diffusion [18], Cones2 [20], OMG [17], and Nested Attention [22]—further reveal persistent identity entanglement, occlusion, and interference when multiple user-defined concepts are composed.

However, recent compositional benchmarks and feedback-driven analyses [7, 35] demonstrate that diffusion models still struggle with relational consistency and fine-grained concept grounding. While these approaches focus on architectural modifications and attention mechanisms, our work identifies visual diversity disparity in training data as a root cause of systematic concept dominance in multi-concept generation.

3. The Dominant-vs-Dominated Phenomenon

3.1. Phenomenon Definition

Multi-concept generation is a fundamental capability of text-to-image diffusion models, enabling users to compose complex scenes from textual descriptions. While recent work has explored training data influence through memorization studies [3, 33, 37] and compositional generation through concept editing [2, 10], we observe a distinct failure mode that operates at the concept level through visual dominance.

We define the *Dominant-vs-Dominated* (DvD) phenomenon as cases where one concept (the *dominant*) visually overwhelms the generation while the other (the *dominated*) is completely suppressed and fails to appear.

Illustrative example. As illustrated in Fig. 1, the prompt “Neuschwanstein Castle coaster” demonstrates this phenomenon: across multiple random seeds, the Castle’s distinctive architecture dominates the generation while the coaster concept is suppressed. This pattern persists across different model versions (SD 1.4 and SD 2.1), indicating that DvD reflects a fundamental issue in diffusion-based generation rather than a model-specific artifact.

Hypothesis: visual diversity disparity. We hypothesize that DvD stems from the disparity in visual diversity across concepts in training data. To investigate this, we examine training images from the LAION [31] dataset for both concepts (Fig. 2). As shown in Fig. 2a, Neuschwanstein Castle, being a unique landmark, appears with highly consistent visual features—the iconic white facade, pointed towers,



Figure 2. Training data examples from LAION. Neuschwanstein Castle exhibits minimal visual variation, while coasters appear in diverse forms and contexts.

and alpine setting remain nearly identical across all training images. In contrast, Fig. 2b reveals that coasters exist in diverse forms: round plates, square tiles, and decorative pieces with various colors, patterns, and materials.

This disparity in training data diversity leads diffusion models to develop internal visual representations with different levels of flexibility. Concepts with limited visual variation—such as famous landmarks, specific artists, or iconic characters—form strongly reinforced, rigid visual priors during training, while concepts with high diversity develop more flexible, adaptable representations. When such concepts are combined in a multi-concept prompt, the rigid priors tend to dominate the generation process, overwhelming and suppressing the more flexible concept.

3.2. Quantification Metric

To quantify the degree of dominance, we define the DvD Score as a metric based on visual presence assessment. For a two-concept prompt, each concept is evaluated through N binary questions using Qwen2.5-VL [1]. Let C_1 and C_2 denote the number of “Yes” responses for the two concepts. The DvD Score is defined as:

$$\text{DvD Score} = \frac{C_1 \times (N - C_2)}{N^2} \times 100. \quad (1)$$

This metric ranges from 0 to 100, with higher values indicating stronger dominance. We set $N = 5$ with concept-type-specific questions (e.g., for artists: “Is this image painted in the artistic style of Van Gogh?”) and consider a prompt as DvD when $C_1 \geq 3$ and $C_2 < 3$ (DvD Score ≥ 36). The complete set of questions is provided in the Appendix.

3.3. DominanceBench

To systematically investigate the causes and mechanisms of DvD, we propose DominanceBench by collecting prompts from the LAION dataset [31], on which SD was trained. We focus on prompts containing two concepts: one from low-diversity groups (artist, landmark, character) and one from a

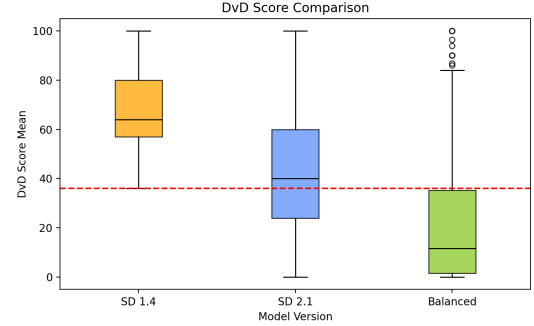


Figure 3. Comparison of mean DvD Scores between SD 1.4 and 2.1. Each box represents the distribution of mean DvD Scores across prompts (10 images per prompt). The red dashed line indicates the DvD Score threshold of 36.

high-diversity group (object, including everyday items such as bags, mugs, and t-shirts). We collect 300 prompts in total, with 100 prompts for each pairing type.

For each prompt, we generate 10 images using SD 1.4 with different random seeds. We compute the DvD Score for each generated image and include a prompt in DominanceBench if at least 7 out of 10 images exceed the threshold of 36.

While the initial collection is performed using SD 1.4, we also evaluate the same prompts with SD 2.1 to examine whether DvD persists across model versions. As shown in Fig. 3, while the overall DvD Score decreases in SD 2.1, a substantial portion of prompts still exceeds the threshold of 36. To validate this threshold, we also use 300 balanced prompts where both concepts successfully appear in generation (details in Appendix). These balanced prompts show significantly lower DvD Scores (median: 11.6), confirming that our threshold effectively distinguishes DvD cases.

4. Analysis

In this section, we analyze the causes and mechanisms of DvD through controlled experiments and attention analysis on SD 1.4.

4.1. Verifying the Role of Visual Diversity

Takeaway 1

Lower visual diversity leads to stronger dominance. When a concept is learned from limited variations, its representation becomes overfit to specific visual patterns, causing it to dominate other concepts in multi-concept compositions.

In Section 3.1, we hypothesized that DvD stems from the disparity in visual diversity across concepts in training data. To directly test this hypothesis, we conduct a controlled experiment where we systematically manipulate the

visual diversity of a single concept and measure the resulting dominance in multi-concept generation.

Experimental Setup. We fine-tune SD 1.4’s UNet using DreamBooth [29] to learn a new concept token “dvddog” from 120 ImageNet [30] dog images. To systematically control visual diversity, we create six training variants by varying the number of dog breeds: $\mathcal{D}_1, \mathcal{D}_2, \mathcal{D}_4, \mathcal{D}_6, \mathcal{D}_8, \mathcal{D}_{10}$, where the subscript indicates the number of breeds. \mathcal{D}_1 uses all 120 images from a single breed (minimal diversity), while \mathcal{D}_{10} uses 12 images from each of 10 breeds (maximal diversity).

All models are trained for 50 epochs with learning rate 1×10^{-5} . We use the original model (without fine-tuning) as a baseline for comparison.

Evaluation. We construct 50 test prompts pairing “dvddog” with diverse concepts across different compositional scenarios: object co-occurrence (e.g., “a dvddog and a cat”), scene context (e.g., “a man walking with a dvddog”), and style modifiers (e.g., “a dvddog in 3d render”). For each prompt, we generate 10 images per model variant using different random seeds and compute the dominance score, treating “dvddog” as C_1 .

Results. We present two representative examples in Fig. 4. In the first example (Figs. 4a and 4b), only \mathcal{D}_1 exceeds the DvD Score threshold of 36, while all other variants remain below the threshold with balanced concept generation. The second example (Figs. 4c and 4d) shows a more pronounced effect: $\mathcal{D}_1, \mathcal{D}_2$, and \mathcal{D}_4 all exceed the threshold, demonstrating that even moderate diversity reduction can trigger dominance in certain compositional contexts. Across both examples, lower-diversity models exhibit visual outputs where “dvddog” dominates the entire scene, with the paired concept either absent or barely visible. In contrast, higher-diversity models ($\mathcal{D}_8, \mathcal{D}_{10}$, baseline) successfully generate both concepts with balanced presence.

This controlled experiment directly validates our hypothesis: *visual diversity disparity between concepts is the root cause of DvD*. When a concept is learned from limited variations, its representation becomes overfitted to specific visual patterns, causing it to dominate other concepts with higher diversity in multi-concept compositions. Additional examples demonstrating this trend across all 50 test prompts are provided in the Appendix.

4.2. Cross-Attention Dynamics in DvD

Having established that visual diversity disparity causes DvD, we now investigate the internal mechanisms through which this phenomenon manifests during generation by

analyzing cross-attention patterns in prompts from DominanceBench.

4.2.1. Measuring Attention Focus

Takeaway 2

In the first denoising step, high attention focus on the dominating concept’s token in lower-resolution layers strongly correlates with DvD occurrence.

To quantify how strongly the model focuses on specific tokens during early generation stages, we define a *focus score*:

$$\text{Focus}^{(\ell,t)} = \frac{\max_i a_i^{(\ell,t)} - \bar{a}_{\text{others}}^{(\ell,t)}}{H(\mathbf{a}^{(\ell,t)}) / \log_2 N + \epsilon} \quad (2)$$

where $\mathbf{a}^{(\ell,t)} = (a_1^{(\ell,t)}, \dots, a_N^{(\ell,t)})$ represents the cross-attention weights over N prompt tokens at layer ℓ and timestep t (averaged across all spatial positions and attention heads), $\max_i a_i^{(\ell,t)}$ is the maximum attention weight, $\bar{a}_{\text{others}}^{(\ell,t)}$ is the mean of all other attention weights, $H(\mathbf{a}^{(\ell,t)})$ is the entropy of the attention distribution, and ϵ is a small constant for numerical stability.

Intuitively, the focus score measures the ratio of attention concentration on the peak token to the overall dispersion across all tokens. High values indicate strong attention concentration on a single dominating token, while low values indicate attention distributed evenly across multiple tokens.

Experimental Setup. We compute focus scores across all UNet layers during the first denoising step ($t = 50$). To characterize the attention patterns in DominanceBench prompts, we compare DominanceBench prompts with 300 balanced prompts where all concepts are successfully generated without DvD. These balanced prompts have an average DvD Score of 20.64, significantly lower than our threshold of 36.

Results. Fig. 5 shows the mean focus scores across all UNet layers (left) and their aggregations for different layer groups (right). DominanceBench prompts exhibit significantly higher focus scores than balanced prompts across layers 5–10, with lower-resolution layers (layers 8–10) showing the most pronounced difference. The elevated focus scores in these lower-resolution layers suggest that the dominant concept’s semantic representation is prioritized during early semantic-level processing.

To verify that this attention concentration indeed targets the dominating concept’s token, we analyze which token receives the peak attention in lower-resolution layers (layers 8–10). We find that in 249 out of 300 DominanceBench prompts (83%), the dominating concept’s token receives the maximum attention in these semantic layers. This confirms

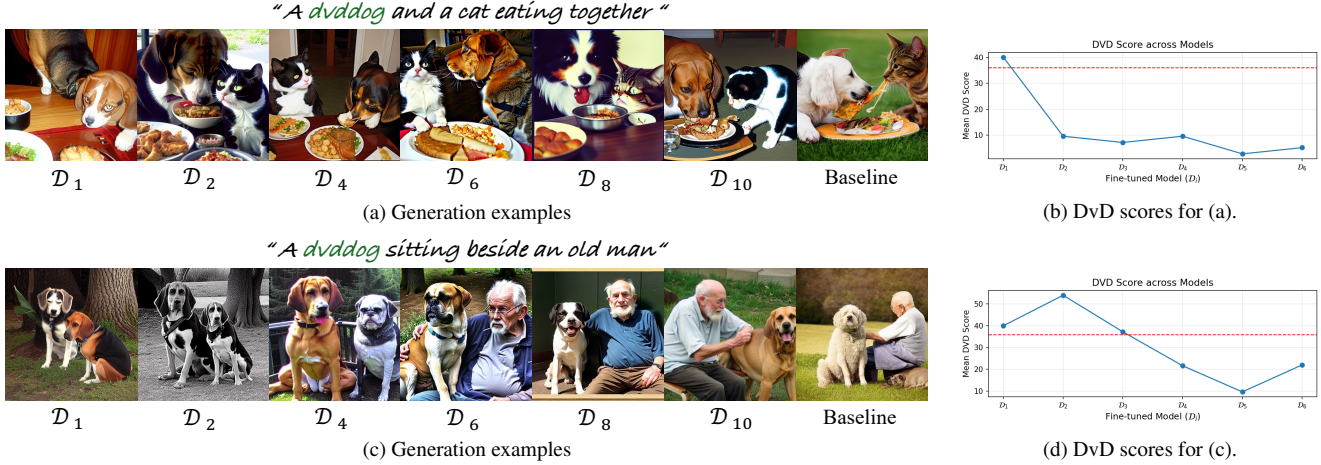


Figure 4. Generation results (left) and DvD scores (right, mean over 10 seeds) for two example prompts across training variants ($\mathcal{D}_1, \mathcal{D}_2, \mathcal{D}_4, \mathcal{D}_6, \mathcal{D}_8, \mathcal{D}_{10}$, baseline). The red dashed line in (b) and (d) indicates the DvD Score threshold of 36.

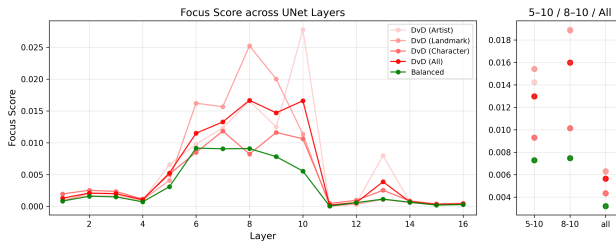


Figure 5. Mean focus scores across UNet layers at the first denoising step for DominanceBench prompts and balanced prompts.

that DvD manifests through *excessive early attention concentration* on the dominating concept’s token in semantic processing layers, preventing adequate attention allocation to other concepts throughout the generation process.

4.2.2. Temporal Analysis of Cross-Attention

Takeaway 3

Dominated concepts rapidly lose attention in early denoising timesteps. In the critical early phase of the generation process, dominated tokens exhibit sharp attention decline while dominating tokens maintain concentration, establishing an imbalance that persists throughout generation.

The focus score analysis revealed that DominanceBench prompts exhibit excessive attention concentration on the dominating concept’s token in lower-resolution layers at the first denoising timestep. But what happens to the dominated concept’s token? Fig. 6 shows the attention patterns for “The Colosseum Rome Italy Carry-all Pouch” and resulting images. Surprisingly, “pouch” exhibits high attention at layer 7 (middle block), where semantic content is

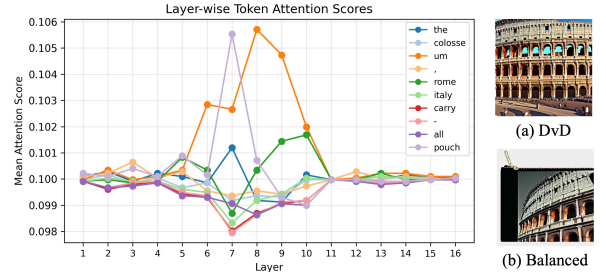


Figure 6. Layer-wise token attention weights at the first denoising timestep for a DominanceBench prompt (“The Colosseum Rome Italy Carry-all Pouch”).

primarily encoded. However, this leads to DvD outcome (Fig. 6a) where only the Colosseum appears, whereas both concepts should appear together as in balanced generation (Fig. 6b). This paradox—high attention yet failed generation—motivates us to examine the temporal dynamics of cross-attention to understand how dominated concepts lose their influence during generation.

Experimental Setup. To understand the temporal dynamics of both concepts, we track each token at the layer where it exhibits peak attention concentration. For the dominating concept, we examine lower-resolution layers (layers 8–10) where high focus scores were observed (Sec. 4.2.1). For the dominated concept, we track layer 7, where the dominated token’s attention exhibits the highest focus score (Fig. 7).

To quantify the temporal evolution of attention for these tokens, we first define the attention deviation for token i at timestep t as $\alpha_i^{(\ell, t)} = a_i^{(\ell, t)} - \bar{a}_{\text{others}}^{(\ell, t)}$ (with the same averaging across spatial positions and heads as in Eq. (2)). Note that we use the raw attention deviation rather than

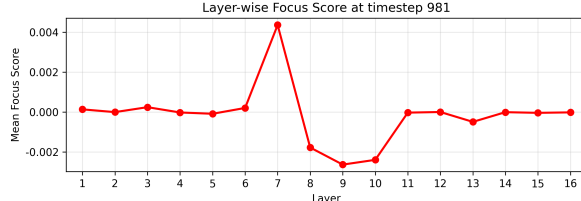


Figure 7. Layer-wise attention distribution for dominated tokens at the first denoising timestep ($t=50$) averaged across all DominanceBench prompts.

the entropy-normalized focus score, as we track dynamics within individual prompts where token count remains constant. Then, the attention change is:

$$\Delta\alpha_i^{(\ell,t)} = \alpha_i^{(\ell,t+1)} - \alpha_i^{(\ell,t)} \quad (3)$$

where we use $\ell \in \{8, 9, 10\}$ (averaged) for dominating tokens and $\ell = 7$ for dominated tokens. Negative $\Delta\alpha$ indicates decreasing concentration on that token.

Results. Fig. 8 shows the temporal evolution of attention change across timesteps. Individual prompts (Fig. 8a,b) and aggregated statistics (Fig. 8c) consistently show that the dominated concept begins with strongly negative $\Delta\alpha$ values in the earliest timestep intervals (50-40), indicating rapid attention loss. In contrast, the dominating concept starts with positive $\Delta\alpha$ values, gaining relative attention in the early phase. This suggests that the attention imbalance is established early and persists throughout generation, with dominated concepts losing their semantic influence in the critical early timesteps where the overall image structure is determined.

4.3. Head Ablation Study

Takeaway 4

DvD arises from distributed attention mechanisms across multiple heads, unlike memorization which localizes to specific heads. This indicates that mitigating DvD requires architectural or training-level interventions rather than simple head pruning.

Our previous analyses revealed that DvD manifests through excessive attention concentration in specific layers during early denoising timesteps. These layer-level findings identified critical layers (e.g., layers 7–10) where dominating and dominated concepts exhibit distinct attention patterns. However, each layer in SD 1.4’s architecture contains 16 attention heads, each potentially contributing differently to the overall layer behavior. This raises an important question: *do all heads within these critical layers equally contribute to DvD, or is the phenomenon driven by specific heads?*

Interestingly, while DvD stems from visual diversity disparity in training data (Sec. 4.1), a related memorization phenomenon also exhibits reduced visual diversity in generated outputs. However, these phenomena differ in crucial ways: memorization affects *individual prompts* that were overfit during training, while DvD occurs in *compositional prompts* where multiple concepts compete for attention. This difference in compositional complexity suggests their underlying attention mechanisms may also differ.

To answer this question and understand how DvD differs from related phenomena, we conduct a head ablation study comparing DvD prompts from DominanceBench with 500 memorized prompts identified in prior work [3]. This comparison allows us to determine whether these phenomena arise from similar mechanisms (both localized or both distributed) or exhibit different head-level characteristics.

Head Ablation Procedure. To assess each head’s contribution, we selectively suppress target heads by scaling their attention logits (pre-softmax scores) with a small factor. Formally, for layer ℓ at timestep t , the ablated attention logit for head h is:

$$\tilde{a}^{(\ell,h,t)} = \begin{cases} \varepsilon \cdot a^{(\ell,h,t)}, & \text{if } \ell = \ell^*, t = t^*, h \in \mathcal{H}^*, \\ a^{(\ell,h,t)}, & \text{otherwise,} \end{cases} \quad (4)$$

where $a^{(\ell,h,t)} \in \mathbb{R}^{P \times N}$ are the attention logits for head h over P spatial positions and N text tokens, ℓ^* is the target layer, t^* is the target timestep, $\mathcal{H}^* \subseteq \{1, \dots, H\}$ is the set of ablated heads, and $\varepsilon = 10^{-5}$ is a small scaling factor that effectively nullifies the head’s influence without disrupting the attention mechanism.

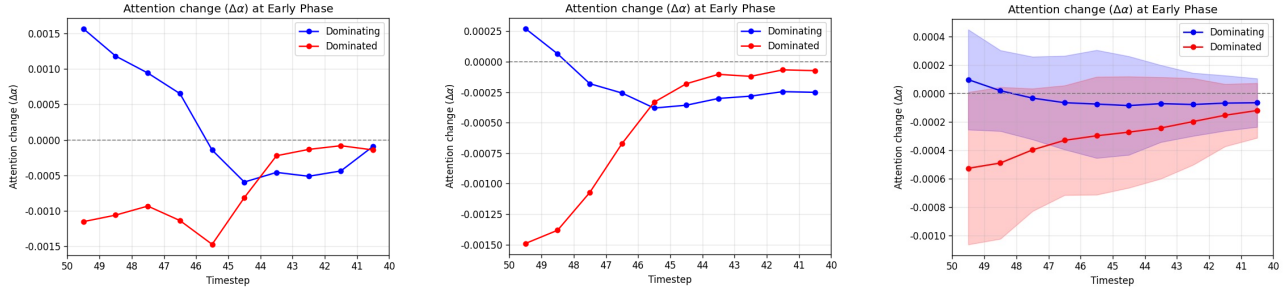
We perform ablation at the first denoising timestep ($t = 50$) across layers 1–16.

Outcome Classification. For each ablated generation, we classify the result into three categories based on visual similarity and task-specific metrics (Fig. 9):

- **Mitigated:** The phenomenon is successfully reduced.
 - *Memorization:* $\text{SSCD} [23] < 0.5$ and $\text{LPIPS} [40] > 0.6$
 - *DvD:* $\text{LPIPS} > 0.5$ and $\text{DvD Score} < 36$
- **Unchanged:** The original unablated behavior persists.
 - *Memorization:* $\text{SSCD} \geq 0.5$ or $\text{LPIPS} \leq 0.6$
 - *DvD:* $\text{LPIPS} \leq 0.5$ or $\text{DvD Score} \geq 36$
- **Others:** The image is severely degraded or incoherent.

4.3.1. Single-Head Ablation

We first ablate individual heads by setting $|\mathcal{H}^*| = 1$ in Eq. (4). For each prompt $p \in \mathcal{P}$ (where \mathcal{P} contains 300 DominanceBench prompts or 500 memorization prompts), we test all heads $h \in \{1, \dots, 16\}$ across all layers.



(a) Van Gogh Two Cut Sunflowers Magnet

(b) Times Square II (B&W widescreen) Notebook

(c) All DominanceBench Prompts

Figure 8. Attention change ($\Delta\alpha$) across timestep intervals. The dominated concept (red) exhibits consistently negative values from the earliest timesteps, while the dominating concept (blue) maintains positive or near-zero values initially.

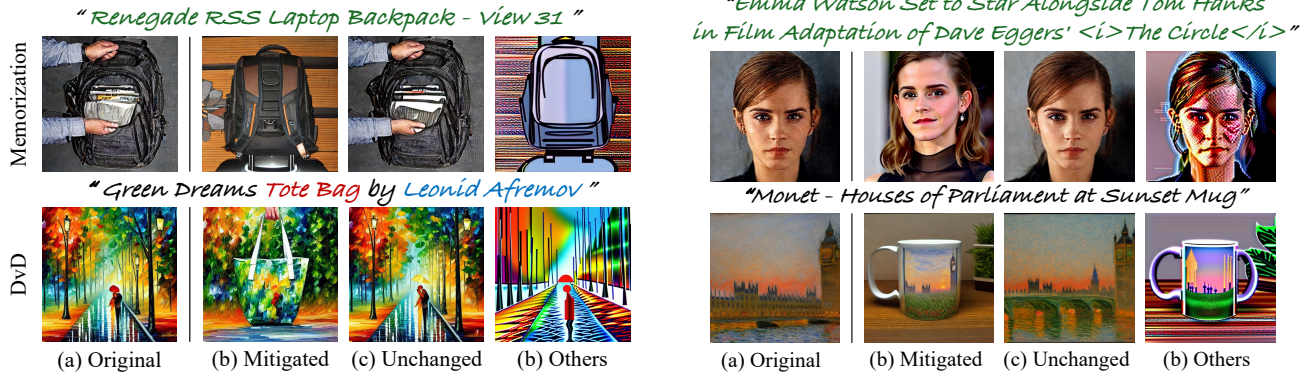


Figure 9. Examples of ablation outcomes across two different settings. From left to right within each panel: (a) Original unablated image, (b) Mitigated (phenomenon reduced), (c) Unchanged (original behavior persists), (d) Others (severely corrupted or incoherent image). The left and right panels correspond to different layer/head configurations for comparison.

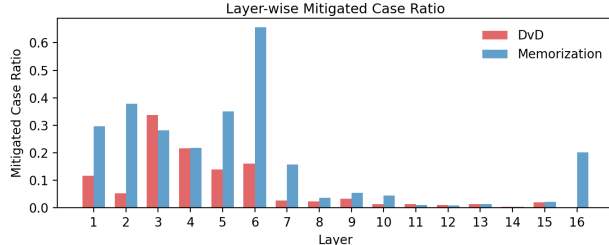


Figure 10. Layer-wise ratio of mitigated cases in single-head ablation. For each layer, the plot shows the proportion of prompts that can be mitigated by ablating at least one head in that layer. Mitigation effects concentrate primarily in layers 1-6 (downsampling blocks) for both phenomena.

Results. Overall, single-head ablation mitigates 145 out of 300 DominanceBench prompts (48%) compared to 392 out of 500 memorization prompts (78%). This substantial difference suggests that memorization is more susceptible to single-head interventions.

As shown in Fig. 10, both phenomena exhibit concentrated effects in layers 1-6 (downsampling blocks), with minimal effects in layers 7-15. Memorization shows a unique spike in layer 16, while DvD remains negligible in

higher layers. Within the critical layers 1-6, memorization achieves its highest mitigation rate at layer 6 (66%), while DvD peaks earlier at layer 3 (22%).

However, these single-head ablation results alone cannot distinguish whether the phenomena arise from localized mechanisms (few critical heads working independently) or distributed mechanisms (collaborative behavior across multiple heads). If the mechanisms are localized, ablating multiple heads simultaneously should maintain high mitigation rates; if distributed, other heads may compensate, reducing the mitigation effect. To determine the underlying mechanistic structure, we conduct multi-head ablation analysis in Sec. 4.3.2.

4.3.2. Multi-Head Ablation

While single-head ablation showed that both phenomena can be mitigated by individual heads, it cannot reveal whether the underlying mechanisms are localized or distributed. To determine whether DvD and memorization arise from localized mechanisms (few critical heads working independently) or distributed mechanisms (collaborative behavior across multiple heads), we conduct multi-head ablation.

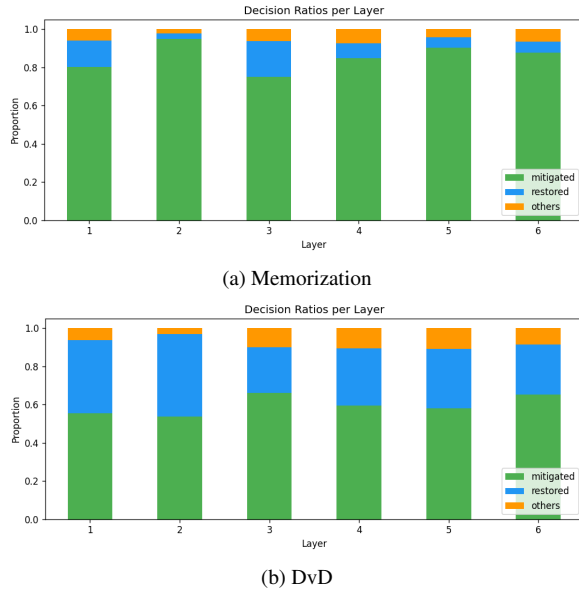


Figure 11. Multi-head ablation outcome proportions across layers 1–6 for memorization (a) and DvD (b).

For each head h that showed mitigation effects in single-head ablation, we simultaneously ablate it with another head h' in the same layer:

$$\mathcal{H}^* = \{h, h'\}, \quad h \neq h'. \quad (5)$$

The ablation procedure follows Eq. (4) with $|\mathcal{H}^*| = 2$. Each ablated image is classified using the same criteria, and we compute the average proportion of each outcome type.

For layer ℓ , the proportion of outcome type $\tau \in \{\text{mitigated, unchanged, others}\}$ is:

$$R_\tau^{(\ell)} = \frac{1}{|\mathcal{P}|} \sum_{p \in \mathcal{P}} \frac{M_\tau^{(\ell)}(p)}{T^{(\ell)}(p)}, \quad (6)$$

where $M_\tau^{(\ell)}(p)$ is the number of head pairs (h, h') in prompt p at layer ℓ that resulted in outcome τ , and $T^{(\ell)}(p)$ is the total number of evaluated head pairs for that prompt and layer. By definition, the three outcome proportions sum to one:

$$R_{\text{mitigated}}^{(\ell)} + R_{\text{unchanged}}^{(\ell)} + R_{\text{others}}^{(\ell)} = 1. \quad (7)$$

Results. Fig. 11 shows the outcome proportions for memorization (a) and DvD (b) across layers. For memorization, the mitigated proportion remains high (~ 0.8) even with multi-head ablation, indicating localized behavior in a few critical heads. In stark contrast, DvD shows lower mitigation proportion (~ 0.6) and higher unchanged proportion (~ 0.2), revealing that it emerges from distributed cooperation among heads—ablation multiple heads simultaneously is less effective because the dominance behavior is not concentrated in specific heads but spread across the network.

This finding reveals a fundamental mechanistic difference: **DvD arises from distributed attention patterns across multiple heads**, while memorization concentrates in specific heads. This distributed nature explains why DvD is more challenging to mitigate through simple head pruning and suggests that addressing it requires broader architectural interventions.

Connection to neuron-level memorization. Recent work on neuron-level memorization [11] provides supporting evidence for our head-level observations. It demonstrated that memorization of individual training samples can be traced to single neurons or small neuron groups within value projection layers. Our finding that memorization localizes to specific heads is consistent with this: the critical neurons they identified are likely concentrated within specific heads rather than distributed across all heads. Conversely, DvD’s resistance to multi-head ablation (Fig. 11b) suggests that its underlying neurons are scattered across multiple heads, requiring distributed coordination.

5. Conclusion

This work analyzed the Dominant-vs-Dominated (DvD) phenomenon in text-to-image diffusion models, where one concept overwhelms multi-concept generation while others are suppressed. We propose DominanceBench, a benchmark of 300 prompts for systematic analysis. Our investigation establishes that visual diversity disparity in training data is the root cause: concepts with limited variation develop rigid visual priors that dominate generation. Cross-attention analysis revealed that DvD emerges through excessive attention concentration on dominating tokens in lower-resolution layers during early denoising steps, with dominated concepts experiencing dramatic attention suppression. Crucially, head ablation studies showed that DvD arises from distributed cooperation among multiple attention heads, contrasting with memorization’s localization to specific heads. This work identifies visual diversity disparity as a previously unexplored cause of multi-concept generation failures, revealing concept-level dominance as a distinct failure mode.

Limitations. Our analysis focused on cross-attention mechanisms as the primary lens for understanding DvD. Investigating feedforward networks and residual connections may reveal additional pathways through which visual diversity disparity affects generation. Additionally, exploring inter-head relationships could provide deeper insights and enable more effective mitigation strategies.

References

[1] Shuai Bai, Kebin Chen, Xuejing Liu, Jialin Wang, Wenbin Ge, Sibo Song, Kai Dang, Peng Wang, Shijie Wang, Jun Tang, et al. Qwen2. 5-vl technical report. *arXiv preprint arXiv:2502.13923*, 2025. 3

[2] Tim Brooks, Aleksander Holynski, and Alexei A Efros. Instructpix2pix: Learning to follow image editing instructions. In *Proceedings of the IEEE/CVF conference on computer vision and pattern recognition*, pages 18392–18402, 2023. 1, 2

[3] N. Carlini, J. Hayes, M. Nasr, M. Jagielski, V. Sehwag, F. Tramèr, B. Balle, D. Ippolito, and E. Wallace. Extracting training data from diffusion models. In *USENIX Security Symposium*, 2023. 1, 2, 6, 12

[4] H. Chefer, Y. Alaluf, Y. Vinker, L. Wolf, and D. Cohen-Or. Attend-and-excite: Attention-based semantic guidance for text-to-image diffusion models. In *Proceedings of the Special Interest Group on Computer Graphics and Interactive Techniques Conference Conference Papers*, 2023. 2

[5] C. Chen, D. Liu, M. Shah, and C. Xu. Exploring local memorization in diffusion models via bright ending attention. In *International Conference on Learning Representations*, 2025. 1, 2

[6] Guillaume Couairon, Jakob Verbeek, Holger Schwenk, and Matthieu Cord. Diffedit: Diffusion-based semantic image editing with mask guidance. In *The Eleventh International Conference on Learning Representations*, 2023. 2

[7] D. Dat, H. Nam, P. Mao, and T. Oh. Vsc: Visual search compositional text-to-image diffusion model. In *Proceedings of the IEEE/CVF International Conference on Computer Vision*, 2025. 2

[8] G. Ding, C. Zhao, W. Wang, Z. Yang, Z. Liu, H. Chen, and C. Shen. Freecustom: Tuning-free customized image generation for multi-concept composition. In *Proceedings of the IEEE/CVF Conference on Computer Vision and Pattern Recognition*, 2024. 1, 2

[9] P. Esser, S. Kulal, A. Blattmann, R. Entezari, J. Müller, H. Saini, Y. Levi, D. Lorenz, A. Sauer, F. Boesel, D. Podell, T. Dockhorn, Z. English, K. Lacey, A. Goodwin, Y. Marek, and R. Rombach. Scaling rectified flow transformers for high-resolution image synthesis. In *International Conference on Machine Learning*, 2024. 1

[10] Amir Hertz, Ron Mokady, Jay Tenenbaum, Kfir Aberman, Yael Pritch, and Daniel Cohen-or. Prompt-to-prompt image editing with cross-attention control. In *The Eleventh International Conference on Learning Representations*, 2023. 1, 2

[11] D. Hintersdorf, L. Struppek, K. Kersting, A. Dziedzic, and F. Boenisch. Finding nemo: Localizing neurons responsible for memorization in diffusion models. In *Advances in Neural Information Processing Systems*, 2024. 1, 2, 8

[12] D. Jeon, D. Kim, and A. No. Understanding memorization in generative models via sharpness in probability landscapes. In *International Conference on Machine Learning*, 2025. 1

[13] J. Jeong, S. Han, J. Kim, and S. Kim. Latent space super-resolution for higher-resolution image generation with diffusion models. In *Proceedings of the IEEE/CVF Conference on Computer Vision and Pattern Recognition*, 2025. 1

[14] J. Jiang, Y. Zhang, K. Feng, X. Wu, W. Li, R. Pei, F. Li, and W. Zuo. Mc²: Multi-concept guidance for customized multi-concept generation. In *Proceedings of the IEEE/CVF Conference on Computer Vision and Pattern Recognition*, 2025. 2

[15] J. Kim, S. Kim, and J.-S. Lee. How diffusion models memorize. *arXiv preprint arXiv:2509.25705*, 2025. 1, 2

[16] Z. Kong, Y. Zhang, T. Yang, T. Wang, K. Zhang, B. Wu, G. Chen, W. Liu, and W. Luo. Compositional generation with energy-based diffusion models. In *International Conference on Machine Learning*, 2023. 2

[17] Z. Kong, Y. Zhang, T. Yang, T. Wang, K. Zhang, B. Wu, G. Chen, W. Liu, and W. Luo. Omg: Occlusion-friendly personalized multi-concept generation in diffusion models. In *European Conference on Computer Vision*, 2024. 2

[18] N. Kumari, B. Zhang, R. Zhang, E. Shechtman, and J. Y. Zhu. Multi-concept customization of text-to-image diffusion. In *Proceedings of the IEEE/CVF Conference on Computer Vision and Pattern Recognition*, 2023. 2

[19] N. Liu, S. Li, Y. Du, A. Torralba, and J. B. Tenenbaum. Compositional visual generation with composable diffusion models. In *European Conference on Computer Vision*, 2022. 2

[20] Z. Liu, Y. Zhang, Y. Shen, K. Zheng, K. Zhu, R. Feng, Y. Liu, D. Zhao, J. Zhou, and Y. Cao. Customizable image synthesis with multiple subjects. In *Advances in Neural Information Processing Systems*, 2023. 2

[21] A. Nichol, P. Dhariwal, A. Ramesh, P. Shyam, P. Mishkin, B. McGrew, I. Sutskever, and M. Chen. Glide: Towards photorealistic image generation and editing with text-guided diffusion models. In *International Conference on Machine Learning*, 2022. 1

[22] O. Patashnik, R. Gal, D. Ostashev, S. Tulyakov, K. Aberman, and D. Cohen-Or. Nested attention: Semantic-aware attention values for concept personalization. In *Proceedings of the Special Interest Group on Computer Graphics and Interactive Techniques Conference Conference Papers*, 2025. 1, 2

[23] Ed Pizzi, Sreya Dutta Roy, Sugosh Nagavara Ravindra, Priya Goyal, and Matthijs Douze. A self-supervised descriptor for image copy detection, 2022. 6

[24] D. Podell, Z. English, K. Lacey, A. Blattmann, T. Dockhorn, J. Müller, J. Penna, and R. Rombach. Sdxl: Improving latent diffusion models for high-resolution image synthesis. In *International Conference on Learning Representations*, 2024. 1

[25] A. Ramesh, M. Pavlov, G. Goh, S. Gray, C. Voss, A. Radford, M. Chen, and I. Sutskever. Zero-shot text-to-image generation. In *International Conference on Machine Learning*, 2021. 1

[26] J. Ren, Y. Li, S. Zeng, H. Xu, L. Lyu, Y. Xing, and J. Tang. Unveiling and mitigating memorization in text-to-image diffusion models through cross attention. In *European Conference on Computer Vision*, 2024. 1, 2, 12

[27] Robin Rombach, Andreas Blattmann, Dominik Lorenz, Patrick Esser, and Björn Ommer. High-resolution image synthesis with latent diffusion models, 2022. 1

[28] B. Ross, H. Kamkari, T. Wu, R. Hosseinzadeh, Z. Liu, G. Stein, J. Cresswell, and G. Loaiza-Ganem. A geometric framework for understanding memorization in generative models. In *International Conference on Learning Representations*, 2025. 1, 2

[29] Nataniel Ruiz, Yuanzhen Li, Varun Jampani, Yael Pritch, Michael Rubinstein, and Kfir Aberman. Dreambooth: Fine tuning text-to-image diffusion models for subject-driven generation. In *Proceedings of the IEEE/CVF conference on computer vision and pattern recognition*, pages 22500–22510, 2023. 1, 4

[30] O. Russakovsky, J. Deng, H. Su, J. Krause, S. Satheesh, S. Ma, Z. Huang, A. Karpathy, A. Khosla, M. Bernstein, A. C. Berg, and L. Fei-Fei. Imagenet large scale visual recognition challenge. *International Journal of Computer Vision*, 115(3):211–252, 2015. 4

[31] Christoph Schuhmann, Romain Beaumont, Richard Vencu, Cade Gordon, Ross Wightman, Mehdi Cherti, Theo Coombes, Aarush Katta, Clayton Mullis, Mitchell Wortsman, et al. Laion-5b: An open large-scale dataset for training next generation image-text models. *Advances in neural information processing systems*, 35:25278–25294, 2022. 2, 3

[32] G. Somepalli, V. Singla, M. Goldblum, J. Geiping, and T. Goldstein. Diffusion art or digital forgery? investigating data replication in diffusion models. In *Proceedings of the IEEE/CVF conference on computer vision and pattern recognition*, 2023. 1

[33] G. Somepalli, V. Singla, M. Goldblum, J. Geiping, and T. Goldstein. Understanding and mitigating copying in diffusion models. In *Advances in Neural Information Processing Systems*, 2023. 1, 2

[34] Z. Tang, Z. Yang, C. Zhu, M. Zeng, and M. Bansal. Any-to-any generation via composable diffusion. In *Advances in Neural Information Processing Systems*, 2023. 2

[35] Y. Wan and K.-W. Chang. Compalign: Improving compositional text-to-image generation with a complex benchmark and fine-grained feedback. *arXiv preprint arXiv:2505.11178*, 2025. 2

[36] S. Wen, G. Fang, R. Zhang, P. Gao, H. Dong, and D. Metaxas. Improving compositional text-to-image generation with large vision-language models. *arXiv preprint arXiv:2310.06311*, 2023. 2

[37] Y. Wen, X. Zhang, Y. Li, Y. Wang, Z. Chen, Y. Chen, X. Zhang, and H. Wang. Detecting, explaining, and mitigating memorization in diffusion models. In *International Conference on Learning Representations*, 2024. 1, 2, 12

[38] C. Zhang, C. Zhang, M. Zhang, and I. S. Kweon. Text-to-image diffusion models in generative ai: A survey. *arXiv preprint arXiv:2303.07909*, 2023. 1

[39] L. Zhang, A. Rao, and M. Agrawala. Adding conditional control to text-to-image diffusion models. In *Proceedings of the IEEE/CVF International Conference on Computer Vision*, 2023. 1

[40] Richard Zhang, Phillip Isola, Alexei A. Efros, Eli Shechtman, and Oliver Wang. The unreasonable effectiveness of deep features as a perceptual metric, 2018. 6

Dominating vs. Dominated: Generative Collapse in Diffusion Models

Supplementary Material

Contents

| | |
|---|----|
| A. DominanceBench | 11 |
| A.1. Training Data Diversity Analysis | 11 |
| A.2. Prompt Collection and Evaluation Details | 11 |
| B. Balanced Prompts | 12 |
| C. Memorized Prompts | 12 |
| D. Additional Results for Sec. 4.1 | 13 |
| D.1. Additional Generation Examples | 13 |
| D.2. Aggregate Results Across All Prompts | 13 |
| D.3. VQA Questions for DvD Score Computation .. | 13 |
| E. Metric Design for Temporal Analysis | 14 |
| E.1. Different Objectives Require Different Metrics | 14 |
| E.2. Entropy Causes Noise in Temporal Analysis .. | 14 |
| E.3. Additional Layer-Wise Consideration | 15 |
| F. Multi-Head Ablation: Additional Results | 15 |
| G. DvD Phenomenon Detection | 15 |
| G.1. Detection Methodology | 16 |
| G.2. Optimal Detection Configuration | 16 |
| G.3. Validation of Detection Accuracy | 16 |
| G.4. Limitations and Future Work | 16 |

A. DominanceBench

A.1. Training Data Diversity Analysis

DominanceBench (Sec. 3.3) categorizes artists, landmarks, and characters as low-diversity concepts and everyday objects as high-diversity based on the visual diversity disparity hypothesis. Here, we empirically verify this categorization by directly analyzing the visual diversity of LAION training images for each concept in Table S1.

To quantify visual diversity, we collect LAION training images associated with the top-k most frequent prompts per concept keyword. We first rank all LAION captions (length 20–100 characters) that contain the keyword, keep the top-k prompts, and download the training images linked to those prompts via their URLs. We then compute CLIP ViT-L/14 image embeddings and measure intra-category cosine distances to assess visual compactness.

Fig. S1 shows the cosine distance distribution for each category. Landmark images exhibit the lowest median distance (0.3079), forming the most compact cluster in the

Table S1. Concept sets used to collect DominanceBench prompts.

| Category | Terms |
|-----------|--|
| Artist | Amedeo Modigliani, Andy Warhol, Camille Pissarro, Caravaggio, Claude Monet, Edgar Degas, Edvard Munch, Egon Schiele, Frida Kahlo, Gustav Klimt, Hokusai, Kandinsky, Leonardo da Vinci, Leonid Afremov, Monet, Pierre-Auguste Renoir, Raphael, Rembrandt, Titian, Van Gogh, Vermeer |
| Character | Barbie, Batman, Black Panther, Buzz Lightyear, Captain America, Cinderella, Goku, Hello Kitty, Hulk, Iron Man, Joker, Luffy, Mickey Mouse, Minions, Naruto, Pikachu, Rapunzel, Simpson, Spider-Man, Superman, Thor, Wonder Woman, Woody |
| Landmark | Acropolis, Big Ben, Brandenburg Gate, Colosseum, Eiffel Tower, Empire State Building, Golden Gate Bridge, Grand Canyon, Great Wall of China, Hagia Sophia, Kremlin, Machu Picchu, Neuschwanstein Castle, Parthenon, Petra, Pyramid, Space Needle, Taj Mahal, Times Square, Tower Bridge |
| Object | Apron, Bag, Battery Charger, Bottle, Canvas Bag, Carry-All Pouch, Clock, Coaster, Coffee Mug, Cup, Curtain, Halloween, Headphones, Hoodie, Lamp, Magnet, Magnets, Mouse Pad, Mousepad, Mug, Necklace, Notebook, Placemat, Pouch, Rug, Sleeves, Spiral Notebook, Sweatshirt, T-Shirt, Tattoo, Tie, Tote Bag, Umbrella, Wallet |

Algorithm 1 DominanceBench Prompt Filtering

```

1: Collect prompts  $p(c, o)$  from LAION dataset of length 20–50
   characters that contain  $c \in (\mathcal{A} \cup \mathcal{C} \cup \mathcal{L})$  and  $o \in \mathcal{O}$ .
2: for each prompt  $p$  do
3:   Generate 10 images  $\{I_1, \dots, I_{10}\}$  using SD 1.4 with dif-
   ferent random seeds.
4:   Compute DvD score for each image  $I_i$ .
5:   Count  $n = |\{i : \text{DvD score}(I_i) > 36\}|$ 
6:   if  $n \geq 7$  then
7:     Add prompt  $p$  to DominanceBench.
8:   end if
9: end for

```

CLIP space with limited visual variation. Character images show moderate compactness (median 0.4417), while artist images (median 0.4660) and everyday object images (median 0.4672) display substantially higher intra-category distances, indicating greater visual diversity.

This image-level analysis validates that the categorization used in DominanceBench construction accurately reflects the actual visual diversity of training data.

A.2. Prompt Collection and Evaluation Details

DominanceBench prompts rely on four concept sets: \mathcal{A} (artist), \mathcal{C} (character), \mathcal{L} (landmark), and \mathcal{O} (object). Table S1 enumerates their elements, and we denote the complete vocabulary as $\mathcal{V} = \mathcal{A} \cup \mathcal{C} \cup \mathcal{L} \cup \mathcal{O}$. The prompt collection procedure is summarized in Algorithm 1.

To compute DvD Scores, we use category-specific questions for each concept type. The five questions per category are listed in Table S2.

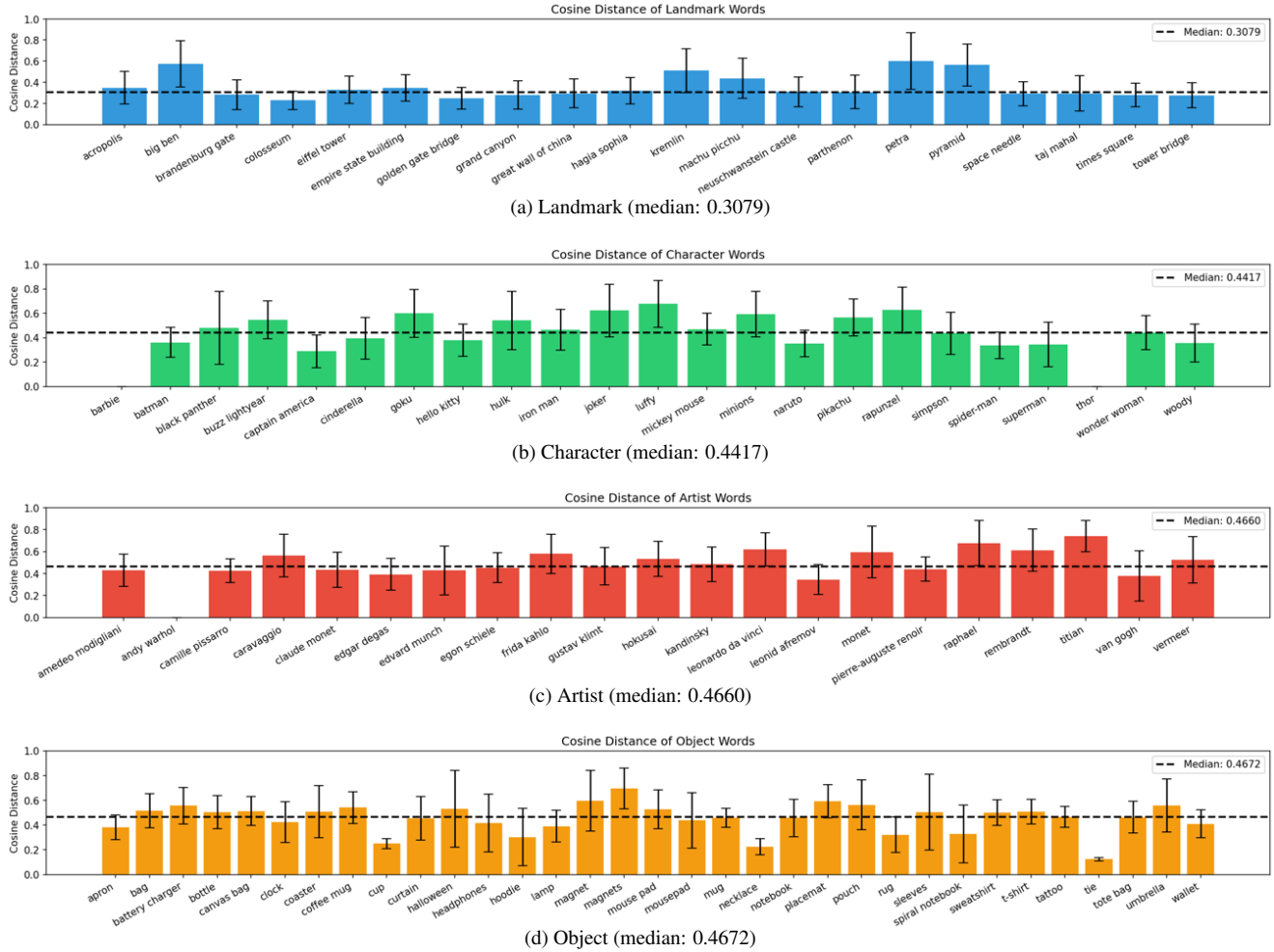


Figure S1. Intra-category cosine distance distributions for LAION training images. For each concept in Table S1, we collected the top 1,000 training images from LAION captions containing that keyword. Lower distances indicate more compact, homogeneous visual clusters. Landmarks show the lowest median distance (0.3079), followed by characters (0.4417), artists (0.4660), and everyday objects (0.4672). We summarize each distribution with the median instead of the mean so that occasional near-duplicate samples, which yield cosine distance 0, do not dominate the statistics.

B. Balanced Prompts

In Sec. 3.3 and Sec. 4.2.1, we use balanced prompts to distinguish DvD behavior from successful multi-concept generation.

We leverage the non-memorized benchmark of Ren et al. [26], which lists 500 everyday prompts curated for memorization studies. We use GPT-5 to identify the number of concepts in each prompt and retain only those with exactly two, yielding 300 prompts. This filtered subset matches the two-concept structure of DominanceBench and covers diverse common concepts.

As shown in Fig. 3, balanced prompts show much lower DvD Scores than DominanceBench. We compute scores using the questions in Table S3 for both concepts, unlike the category-specific questions in Table S2.

C. Memorized Prompts

In Sec. 4.3, we compare DvD with memorization using 500 memorized prompts identified by Carlini et al. [3]. Among existing studies on memorization, Wen et al. [37] proposed a detection method that computes the L2 norm of text-conditional noise predictions at the first denoising step. A higher L2 norm value indicates that the prompt consistently reproduces the same image regardless of the random seed. To further characterize DominanceBench, we apply this metric to compare the three prompt sets.

Fig. S2 shows the L2 norm distributions across memorized prompts, DominanceBench, and balanced prompts. Memorized prompts show the highest values, DominanceBench shows intermediate values, and balanced prompts show the lowest. This intermediate position im-

Table S2. Questions used in collecting DominanceBench for each category.

| Category | Questions |
|----------|---|
| Artist | <ul style="list-style-type: none"> Is this image painted in the artistic style of Artist, using realistic lighting and smooth brush strokes? Does the person or subject look painted with the realistic portrait technique typical of Artist? Does this image show brushwork, color tones, or shading similar to paintings by Artist? Does this look like a painting created by Artist, rather than a photo or modern artwork? Is the visual composition, lighting, and realism clearly similar to Artist's paintings? |
| | <ul style="list-style-type: none"> Does the image show architectural details or a skyline resembling the Landmark? |
| | <ul style="list-style-type: none"> Is the Landmark the main subject or part of the background in this image? Is the Landmark or part of it visible anywhere in the image? Is this a photograph or realistic depiction of the Landmark? Is the structure clearly identifiable as the Landmark? |
| | <ul style="list-style-type: none"> Does the image contain a logo, costume, or any reference to Character? Is the scene related to, inspired by, or set in the world of Character? Is there a visual element or theme in the image connected to Character? Does the person or figure look like Character? Is Character visible in the image? |
| | <ul style="list-style-type: none"> Does this image look like a product photo or include a depiction of a Object? Is there a Object included or partly shown in the image? Is the appearance or shape recognizable as a Object? Does the image feature or focus on a Object? Is a Object visible in the image? |

Table S3. Questions used in calculating DvD Score for balanced prompts.

| Category | Questions |
|----------|--|
| Concept | <ul style="list-style-type: none"> Does the image include Concept as part of the scene? Does the image show Concept in a recognizable way? Is Concept visually represented in the image? Can you see Concept clearly in the image? Is Concept present in the image? |

plies that the dominant concepts (e.g., landmarks, artists) tend to reproduce visually memorized patterns from the training data.

D. Additional Results for Sec. 4.1

In Sec. 4.1, we demonstrated that lower visual diversity leads to stronger dominance through a controlled experiment with six training variants ($\mathcal{D}_1, \mathcal{D}_2, \mathcal{D}_4, \mathcal{D}_6, \mathcal{D}_8, \mathcal{D}_{10}$). Here we provide additional results across all 50 test prompts.

D.1. Additional Generation Examples

Fig. S3 shows five additional examples beyond the two presented in Fig. 4. Lower-diversity models ($\mathcal{D}_1, \mathcal{D}_2$) consist

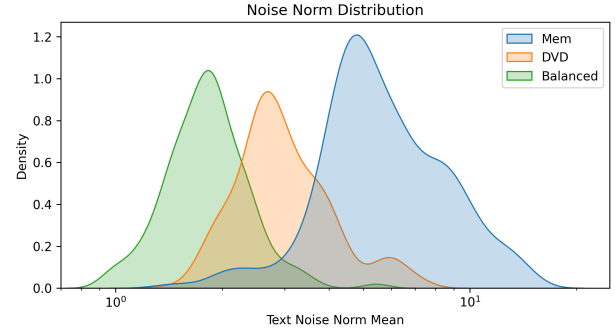


Figure S2. L2 norm distributions of text-conditional noise predictions at the first denoising step across memorized, DominanceBench, and balanced prompts.

Table S4. Questions used to calculate DvD Score. The first set checks whether “dvddog” is present, while the second and third sets verify the paired concept depending on whether it is an object/scene or a style/material.

| Category | Questions |
|------------------------------------|---|
| “dvddog” | <ul style="list-style-type: none"> Is a dog visible in this image? Is the dog fully or partially visible? Is the dog clearly identifiable? Is the dog easy to recognize? Is the dog the main subject of this image? |
| Paired concept (object or scene) | <ul style="list-style-type: none"> Is concept visible in this image, separate from the dog? Is concept fully or partially visible? Is concept clearly identifiable? Is concept unambiguously visible? Is concept appearing together with the dog? |
| Paired concept (style or material) | <ul style="list-style-type: none"> Is the dog shown in the concept style? Does the dog appear made of concept? Is the dog drawn in the concept style? Is the concept style visible on the dog? Does the dog's appearance resemble the concept style? |

tently exceed the DvD Score threshold of 36, while higher-diversity models ($\mathcal{D}_8, \mathcal{D}_{10}$, baseline) generate balanced compositions.

D.2. Aggregate Results Across All Prompts

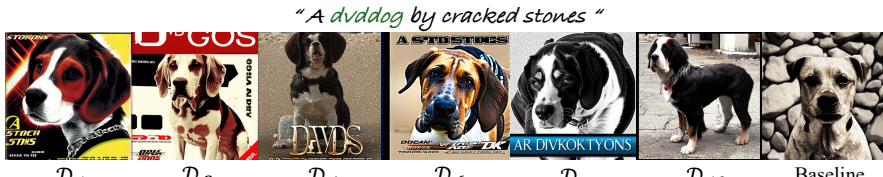
Fig. S4 presents the distribution of DvD Scores across all 50 test prompts for each model variant. Each box plot shows the distribution of mean DvD Scores (averaged over 10 seeds per prompt). The decreasing trend from \mathcal{D}_1 to baseline demonstrates that lower diversity consistently leads to stronger dominance.

D.3. VQA Questions for DvD Score Computation

Table S4 lists the questions used to compute DvD Scores in this experiment. VQA models recognize “dvddog” as a dog in the generated images, so we query for dog presence. For the paired concept, we use type-specific questions depending on whether it is an object/scene or a style/material.



(a) Generation examples



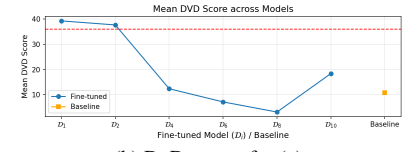
(c) Generation examples



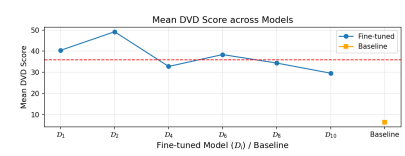
(e) Generation examples



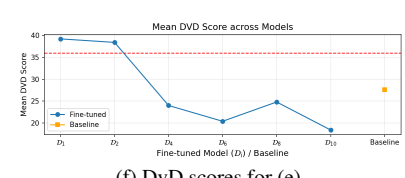
(g) Generation examples



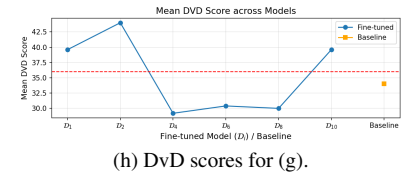
(b) DvD scores for (a).



(d) DvD scores for (c).



(f) DvD scores for (e).



(h) DvD scores for (g).

Figure S3. Generation results (left) and mean DvD scores over 10 seeds (right) for four supplementary prompts across the training variants (D_1 – D_{10} , baseline). Red dashed lines in the score plots mark the DvD threshold of 36. Each row mirrors the structure of Fig. 4, highlighting that reduced training diversity consistently yields higher dominance.

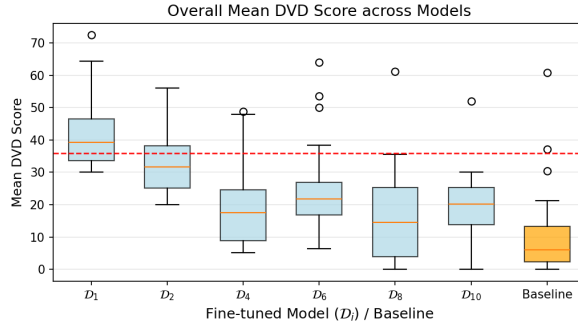


Figure S4. Distribution of mean DvD Scores across all 50 test prompts for each training variant. Each data point represents the mean score over 10 seeds for one prompt. The decreasing trend from D_1 to baseline shows that lower diversity consistently leads to stronger dominance.

E. Metric Design for Temporal Analysis

While the Focus Score (Eq. 2) uses entropy normalization, our Temporal Analysis (Sec. 4.2.2) uses only attention deviation without entropy. We explain why below.

E.1. Different Objectives Require Different Metrics

The Focus Score compares attention patterns across different prompts with varying characteristics. The numerator measures attention concentration on the peak token relative to others, while the denominator uses entropy to capture the overall dispersion of the attention distribution. Normalizing entropy by $\log_2 N$ accounts for prompt length, enabling fair comparison across prompts with different token counts.

In contrast, Temporal Analysis tracks attention dynamics within a single prompt over time. The attention deviation $\alpha_i^{(l,t)} = a_i^{(l,t)} - \bar{a}_{others}^{(l,t)}$ already captures relative token importance, and its temporal change $\Delta\alpha_i^{(l,t)}$ directly measures how the competitive balance shifts between concepts. We do not use entropy normalization because it causes distortion from irrelevant tokens, as explained below.

E.2. Entropy Causes Noise in Temporal Analysis

Entropy H measures the dispersion of the entire attention distribution, including tokens irrelevant to the dominating and dominated concepts (denoted as C_D and C_d ,

Table S5. Attention weights at consecutive timesteps. The attention of C_D and C_d remains constant while that of an irrelevant token T_1 suddenly increases.

| Token | Timestep t | Timestep $t + 1$ | Change |
|-----------------------|--------------|------------------|--------------|
| C_D (Dominating) | 0.40 | 0.40 | 0 |
| C_d (Dominated) | 0.30 | 0.30 | 0 |
| T_1 (Another token) | 0.05 | 0.15 | +0.10 |
| Other 7 tokens | 0.036 each | 0.021 each | -0.015 each |

respectively). When irrelevant tokens shift attention, entropy changes even if the attention to C_D and C_d remains unchanged, leading to distorted interpretations of concept-level dynamics.

As a concrete example, consider 10 tokens (C_D , C_d , and 8 other tokens) with $\sum a_i = 1.0$ (Table S5):

Using attention deviation (our approach):

$$\bar{a}_{\text{others}}^{(t)} = \frac{1 - 0.40}{9} \approx 0.067 \quad (8)$$

$$\bar{a}_{\text{others}}^{(t+1)} = \frac{1 - 0.40}{9} \approx 0.067 \quad (9)$$

$$\alpha_{C_D}^{(t)} = 0.40 - 0.067 = 0.333 \quad (10)$$

$$\alpha_{C_D}^{(t+1)} = 0.40 - 0.067 = 0.333 \quad (11)$$

$$\Delta\alpha_{C_D} = 0 \quad (12)$$

Correct interpretation: C_D ’s relative advantage is unchanged.

If entropy normalization is used hypothetically:

At timestep t , attention is concentrated primarily on C_D (0.40) and C_d (0.30), with other tokens having small weights (e.g., 0.05, 0.0357 each), yielding low H_t . At timestep $t + 1$, attention becomes more distributed as the attention of T_1 increases to 0.15, while those of C_D (0.40) and C_d (0.30) remain constant, yielding higher H_{t+1} .

An entropy-normalized metric would give:

$$\text{Score}_t = \frac{\alpha_{C_D}^{(t)}}{H_t / \log_2 N} \quad (\text{high value}) \quad (13)$$

$$\text{Score}_{t+1} = \frac{\alpha_{C_D}^{(t+1)}}{H_{t+1} / \log_2 N} \quad (\text{lower value}) \quad (14)$$

$$\Delta\text{Score} < 0 \quad (15)$$

Distorted interpretation: “ C_D ’s dominance decreased”—despite a_{C_D} remaining constant at 0.40. This distortion occurs because the entropy increase stems from irrelevant token T_1 (0.05 \rightarrow 0.15), not from changes in the dominating (C_D) or dominated (C_d) concepts that Temporal Analysis aims to isolate.

E.3. Additional Layer-Wise Consideration

Beyond the token-level noise discussed above, incorporating entropy would create an additional issue for cross-layer

tracking. As described in Sec. 4.2.2, we track dominating tokens in layers 8–10 and dominated tokens in layer 7. Since each layer has its own entropy value, any metric involving entropy cannot be directly compared across layers. Attention deviation $\alpha_i^{(l,t)} = a_i^{(l,t)} - \bar{a}_{\text{others}}^{(l,t)}$ isolates relative token importance within each layer, enabling consistent cross-layer comparison.

Summary. By using only attention deviation, our Temporal Analysis (1) maintains direct interpretability ($\Delta\alpha =$ change in relative advantage), (2) eliminates noise from irrelevant tokens, and (3) enables consistent cross-layer tracking of the dominating and dominated concepts that characterize the DvD phenomenon.

F. Ablation on Non-Mitigated Heads

In single-head ablation (Sec. 4.3), some heads showed mitigation effects while others did not. To further examine the role of non-mitigating heads, we perform pairwise ablation within layer 1: for each non-mitigating head, we ablate it together with every other head in the same layer.

Table S6 shows the results. For DvD, the mitigation rate is near zero (0.55%), showing these heads do not directly drive the dominance behavior. However, the Others rate—cases where the outputs become corrupted or fail to depict both concepts as described in Sec. 4.3—reaches 18.68%, nearly twice that of memorization (9.92%). This means that while these heads cannot mitigate DvD on their own, they still help maintain coherent generation. Removing multiple such heads breaks the generation process without fixing the dominance. In contrast, memorization shows a small increase in mitigation rate (2.90%) with lower Others (9.92%), consistent with its localized mechanism where non-mitigating heads have limited involvement.

Table S6. Results of layer-1 multi-head ablation on the heads that did not mitigate the phenomenon in the single-head study. “Maintained” indicates that the original DvD or memorization behavior persisted after ablation.

| Phenomenon | Mitigated | Maintained | Others |
|--------------|--------------|------------|---------------|
| DvD | 0.55% | 80.77% | 18.68% |
| Memorization | 2.90% | 87.18% | 9.92% |

G. DvD Phenomenon Detection

Based on our findings, this section presents a method for detecting DvD in real-time and validates the accuracy of detection. While the main contribution of this paper is identifying the causes and mechanisms of the DvD phenomenon, from a practical perspective, early detection of DvD during generation can serve as a foundation for future mitigation research.

Table S7. Detection rates across different Focus Score thresholds and layer configurations. Values represent the percentage of prompts flagged as DvD. The configuration achieving the maximum discrimination gap is highlighted in bold: threshold 0.010 with layers 9&10 yields 70.67% detection on DominanceBench versus 33.67% on Balanced prompts, producing a gap of 37.00 percentage points.

| Threshold | Layer Configuration | | | | | | | |
|---|---------------------|-------|-------|-------|-------|-------|-------|--------------|
| | max | mean | L8 | L9 | L10 | 8&9 | 8&10 | 9&10 |
| <i>DominanceBench (300 prompts)</i> | | | | | | | | |
| 0.010 | 81.00 | 67.33 | 55.00 | 60.00 | 63.67 | 61.67 | 67.33 | 70.67 |
| 0.015 | 66.00 | 47.67 | 38.00 | 39.33 | 43.33 | 39.00 | 47.00 | 49.00 |
| 0.020 | 54.67 | 27.00 | 28.67 | 25.33 | 33.33 | 26.33 | 35.00 | 27.67 |
| 0.025 | 40.67 | 15.00 | 21.33 | 14.33 | 21.67 | 16.67 | 19.00 | 14.00 |
| <i>Balanced Prompts (300 prompts)</i> | | | | | | | | |
| 0.010 | 62.67 | 41.00 | 52.00 | 40.67 | 26.33 | 48.67 | 38.00 | 33.67 |
| 0.015 | 41.00 | 17.00 | 29.67 | 27.33 | 10.33 | 25.67 | 17.33 | 17.00 |
| 0.020 | 22.67 | 7.67 | 15.33 | 15.00 | 4.00 | 11.67 | 7.00 | 7.67 |
| 0.025 | 11.33 | 5.00 | 8.33 | 7.33 | 2.33 | 6.33 | 3.33 | 3.33 |
| <i>Discrimination Gap (percentage points)</i> | | | | | | | | |
| 0.010 | 18.33 | 26.33 | 3.00 | 19.33 | 37.34 | 13.00 | 29.33 | 37.00 |
| 0.015 | 25.00 | 30.67 | 8.33 | 12.00 | 33.00 | 13.33 | 29.67 | 32.00 |
| 0.020 | 32.00 | 19.33 | 13.34 | 10.33 | 29.33 | 14.66 | 28.00 | 20.00 |
| 0.025 | 29.34 | 10.00 | 13.00 | 7.00 | 19.34 | 10.34 | 15.67 | 10.67 |

G.1. Detection Methodology

We use the Focus Score (Eq. 2) to detect DvD. When the Focus Score exceeds a specific threshold, we determine that the prompt is likely to trigger DvD. Specifically, we compute the Focus Score in lower-resolution layers at the first denoising step ($t = 50$), and identify the token receiving maximum attention as the dominant concept token.

G.2. Optimal Detection Configuration

Based on Sec. 4.2.1 (Fig. 5) showing that DominanceBench prompts exhibit particularly high Focus Scores in layers 8–10, we focus on these specific lower-resolution layers to optimize detection settings. We test various combinations of Focus Score thresholds $\{0.010, 0.015, 0.020, 0.025\}$ and layer configurations (single layers, layer combinations, and aggregation methods), evaluating a total of 32 settings. To balance high detection rate on DvD cases with low false positive rate on balanced prompts, we select the configuration that maximizes the gap between the two detection rates.

Tab. S7 shows the detection rates across all configurations. Higher thresholds reduce false positives on Balanced prompts but also miss many true DvD cases, while lower thresholds with aggressive layer aggregation (e.g., max) detect more DvD cases but produce excessive false positives. Among all settings, a threshold of 0.010 with layer combination 9&10 achieves the optimal balance with the maximum discrimination gap of 37.00 percentage points (70.67% on DominanceBench vs. 33.67% on Balanced).

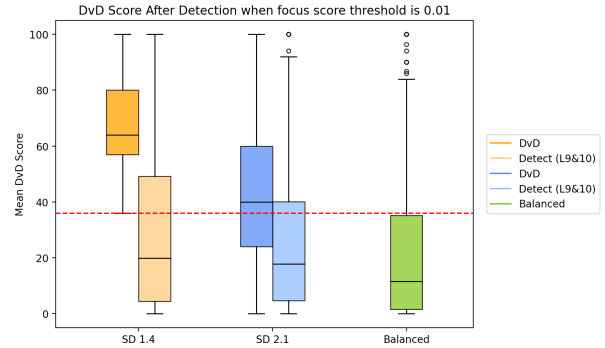


Figure S5. DvD Score distribution before (darker boxes) and after (lighter boxes) replacing detected tokens with generic category terms, using the optimal configuration (threshold 0.010, layers 9&10). Results are shown for DominanceBench prompts on SD 1.4 (orange) and SD 2.1 (blue), with Balanced prompts (green) for reference. The dramatic reduction validates accurate detection of dominant concept tokens. Red dashed line: DvD threshold of 36.

G.3. Validation of Detection Accuracy

To verify whether our detection method accurately identifies dominant concept tokens, we observed changes in DvD Score after modifying the tokens. Specifically, for prompts flagged as DvD by the optimal configuration (threshold 0.010, layers 9&10), we identify the token receiving maximum attention in those layers and modify it.

Based on the visual diversity disparity hypothesis revealed in Sec. 4.1, we replace detected dominant tokens with generic category nouns:

- Artist: Van Gogh → “artist”
- Landmark: Colosseum → “landmark”
- Character: Spider-Man → “character”

If detection is accurate, this modification should reduce the DvD Score by replacing specific, low-diversity concepts with generic, high-diversity terms that allow more flexible representations.

Fig. S5 shows the dramatic reduction in DvD Score distribution after modification. In SD 1.4, the median DvD Score decreased from 64 to 20. In SD 2.1, a similar pattern was observed, with the median decreasing from 40 to approximately 17.

G.4. Limitations and Future Work

The purpose of this section was to validate the accuracy of the detection method, and we clarify that prompt modification itself may not be a practical solution. When a user requests “Van Gogh coaster,” generating “artist coaster” undermines the original intent. Future research should explore architectural modifications or training-level methods that alleviate DvD without modifying prompts. The detection method presented in this section can be used as a diagnostic tool for developing such mitigation methods.